Journal of Photochemistry & Photobiology, A: Chemistry 456 (2024) 115793

Contents lists available at ScienceDirect

Journal of Photochemistry & Photobiology, A: Chemistry

journal homepage: www.elsevier.com/locate/jphotochem

Water modulates the chemiexcitation efficiency of the peroxyoxalate reaction: Enhancement at low and decrease at higher concentrations

Maidileyvis C. Cabello [a,b], Marcos P.O. Lemos [a], Wilhelm J. Baader [a,*]

[a] Departamento de Química Fundamental, Instituto de Química, Universidade de São Paulo, Av. Prof. Lineu Prestes, 748, 05508-000, São Paulo, Brazil
[b] Department of Chemistry, Southern Methodist University, Dallas, TX 75275-0314, United States

ARTICLE INFO

Keywords:
Peroxyoxalate chemiluminescence
Chemiexcitation mechanism
Water effect
Electron transfer
Singlet quantum yields

ABSTRACT

Chemiluminescence transformations are widely utilized in analytical and bioanalytical applications. Specifically, the peroxyoxalate system can be employed for sensitive quantification of a wide variety of analytes. Under anhydrous conditions, the peroxyoxalate reaction shows extremely high emission quantum yields, comparable to highly efficient bioluminescence systems. However, in aqueous media, important for bioanalytical applications, the emission efficiency suffers a significant decrease of several orders of magnitudes, although the reason for this loss in efficiency is unknown up to now.

In the present work, we show the results of a detailed photophysical study on the effect of water on the chemiexcitation efficiency of the peroxyoxalate reaction using bis(2,4-dinitrophenyl) oxalate as reagent and imidazole as base catalyst in the presence of different chemiluminescence activators. It is shown that in 1,2-dimethoxyethane/water mixtures (DME:H_2O), singlet quantum yields increase with increasing the water concentrations up to 0.7 mol/L, followed by a steady decrease at higher water concentrations. The decrease in quantum yields is not predominantly due to concurrent ester hydrolysis, as quantum yields could be corrected for this side reaction. This indicates that the quantum yield decrease is due to the diminished chemiexcitation efficiency in the presence of water. Using different activators, it is shown that chemiexcitation occurs via electron transfer and electron back-transfer steps between a high-energy intermediate and the activator. Additionally, its efficiency is governed by the energetics of the electron back-transfer step, in agreement with the Chemically Initiated Electron Exchange Luminescence (CIEEL) mechanism, also in partially aqueous environment. Lower excitation efficiency in aqueous media may be due to formation of solvent-separated radical ion pairs, inhibiting chemiexcitation.

1. Introduction

The analytical and bioanalytical use of chemiluminescence (CL) is being actively investigated since it represents an easy, inexpensive, and sensitive alternative to quantify a wide variety of compounds [1–6]. Emission intensity measurements can be used for these purposes because it is a function of the concentration of the chemical species present in the sample which lead to light emission [7]. One of the most frequently used chemiluminescent systems is the peroxyoxalate reaction, first described by Edwin A. Chandross, due to its high quantum yield [8]. The system is based on the base-catalyzed reaction of oxalic acid derivatives with hydrogen peroxide in the presence of an appropriate fluorophore, called activator (ACT) (Scheme 1) [9–11].

In general terms, the reaction occurs with the initial formation of a high-energy intermediate (HEI) from the oxalate derivative and hydrogen peroxide, in several base-catalyzed steps, which has shown to be the cyclic peroxidic carbon dioxide dimer 1,2-dioxetanedione [12,13]. In the so-called chemiexcitation step, this HEI interacts with the activator, generally a highly fluorescent compound with low oxidation potential, leading to the formation of the electronically excited singlet state of the ACT. Finally, the singlet-excited ACT is responsible for the observed chemiluminescence corresponding to its fluorescence emission [14].

The reaction steps leading to the formation of the HEI have been well characterized under different reaction conditions; they involve the base-catalyzed cyclization of an oxalic peracid derivative to a cyclic peroxide as the key-step [15–18]. The interaction of the HEI with the ACT in the chemiexcitation step has been shown to occur via electron transfer, and electron back-transfer step according to the Chemically Initiated Electron Exchange Luminescence (CIEEL) [19–22]. The efficiency of these

* Corresponding author.
E-mail address: wjbaader@iq.usp.br (W.J. Baader).

https://doi.org/10.1016/j.jphotochem.2024.115793
Received 3 March 2024; Received in revised form 3 May 2024; Accepted 26 May 2024
Available online 31 May 2024

electron transfer steps for excited state formation is the main factor that determines the quantum yields of the chemiluminescence transformation. The efficiency of the last step, fluorescence emission from the first singlet-excited state of the ACT, is just determined by its fluorescence quantum yield [23–25].

Although the mechanism of the peroxyoxalate reaction has been mainly studied in anhydrous media to avoid reactive ester hydrolysis, several recent studies have shown the possible application of the transformation in aqueous media, due to its importance as an analytical, and bioanalytical tool [14,26–34]. However, the singlet-excitation quantum yields in these aqueous media were found to be several orders of magnitude lower [35–40] when compared to those obtained in anhydrous organic solvents [10,20,41–43]. Until present, no systematic study has been performed to investigate the influence of water on the chemiexcitation efficiency of the peroxyoxalate system, although the use of aqueous media is important per se, as well as for analytical and bioanalytical applications.

In the present work, the effect of water on the efficiency of the peroxyoxalate reaction is studied in the reaction of bis(2,4-dinitrophenyl) oxalate (DNPO) reaction with H_2O_2 and catalyzed by imidazole using different aqueous 1,2-dimethoxyethane as reaction medium. The reason for using this mixed solvent is that the reaction conditions leading to reproducible kinetic data were established for this medium [44]. The determination of the chemiluminescence parameters with different ACTs bears on the effect of water on the efficiency of the chemiexcitation step.

2. Materials and methods

Bis(2,4-dinitrophenyl) oxalate (DNPO, Aldrich), imidazole (IMI-H, Sigma, 99 %), 9,10-diphenylanthracene (DPA), 2,5-diphenyloxazole (PPO), rubrene (RUB), perylene (PER) (all Aldrich) were obtained commercially and used without further purification. 1,2-Dimethoxyethane (DME, Sigma-Aldrich, 99.5 %) was refluxed and distilled from sodium wire in the presence of benzophenone as indicator·H_2O_2 stock solutions were prepared by diluting a 60 % aqueous solution in DME, the residual water being removed by addition of $MgSO_4$ followed by filtration; the final H_2O_2 concentration was determined by photometric iodometry [45]. Aqueous DME with known molar concentration of water was prepared by mass.

Light emission kinetic experiments were performed using 10 mm pathlength fluorescence quartz cuvettes in a Varian Cary Eclipse fluorescence spectrophotometer. The kinetic assays were performed at (25.0 ± 0.5) °C by adding the appropriate amounts of IMI-H, H_2O_2 and ACT stock solutions in DME to the cuvette, containing DME or DME:H_2O mixtures, in a final volume of 2.0 mL. The reaction was started by injecting the appropriate volume of DNPO stock solution in dry DME, followed by emission intensity data acquisition. All experiments were carried out at least in triplicates. Chemiluminescence quantum yields (Φ_{CL}) were determined, using the luminol standard for photomultiplier calibration [20]. The singlet quantum yields (Φ_S) were calculated from the (ΦCL) by using the fluorescence quantum yields of the activators, determined in the reaction medium as absolute quantum yields, for water concentrations of 0.0, 0.22, 0.7 and 1.2 mol/L In DME. The absolute fluorescence quantum yields (Φ_{Fl}) were determined using the integration sphere (SC-30) of the steady state spectrofluorometer Edinburgh FS5, using the software for reabsorption correction integrated to the instrument. For DPA, fluorescence quantum yields were also determined for higher water concentrations, up to 6.5 mol/L (Table S1). The absorption and emission spectra of DPA in binary DME water mixtures with water concentrations of up to 6.5 mol/L do not show significant alterations with the water concentration, indicating that aggregation phenomenon appear not to be important in these conditions (Figures S1 and S2).

The empirical polarities for DME-water binary mixtures, $E_T(33)$ in kcal/mol, were calculated from the values of λ_{max} of the solvent-sensitive (i.e., solvatochromic) peak of the probe 2,6-dichloro-4-(2,4,6-triphenyl-N-pyridinium) phenolate (WB), using UV–Visible spectrophotometry measurements were performed in a Varian Cary 50 Probe spectrophotometer [46]. Aliquots of the WB stock solution (1.3 10^{-3} mol/L in acetone) were pipetted into 2 mL volumetric tubes, followed by evaporation of acetone at room temperature, under reduced pressure, in the presence of P_4O_{10}. DME-water was then added to the (solid) probe, and the latter was dissolved, the solution transferred to the cell and its UV–Vis absorption measured (Table S2). The dependence of the $E_T(33)$ values with the water concentration is clearly not linear, indicating preferential solvation of the zwitterionic probe (Figure S3).

3. Results

The kinetics of the imidazole catalyzed reaction of DNPO with hydrogen peroxide in the presence of DPA as activator was studied by monitoring the decay of the light emission intensity as a function of water concentrations from 0 to almost 7 mol/L. The emission intensity *versus* time curves, adjusted by a mono exponential equation, give rise to observed rate constants (k_{obs}) and the singlet excitation quantum yields (Φ_S), obtained from the integral of the kinetic emission intensity curves (Table S3). The decay rate constants increased with the water concentration; however, they are largely independent of the activator concentration (Fig. 1).

Interestingly, the values of the singlet quantum yield (Φ_s) increase with increasing water concentration, followed by a significant decrease of more than an order of magnitude for higher concentrations. The

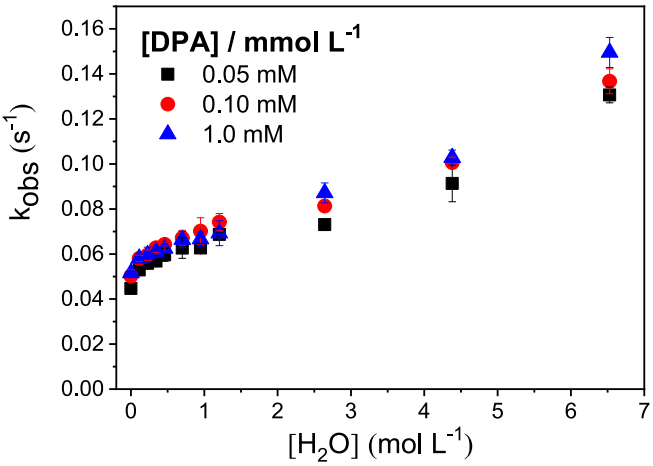

Fig. 1. Dependence of the rate constants (k_{obs}) of the decay of emission intensity on the [H_2O] in the imidazole (0.20 mmol/L) catalyzed reaction of DNPO (0.10 mmol/L) with H_2O_2 (10 mmol/L) in presence of three different DPA concentrations, at 25 °C.

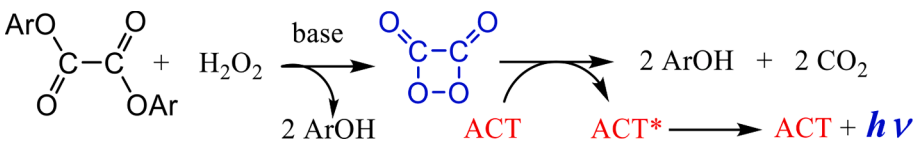

Scheme 1. Peroxyoxalate reaction of an aromatic oxalic ester with hydrogen peroxide in the presence of a base and an activator (ACT).

behavior of the quantum yields is similar for different DPA concentrations; the values of Φ_s start to decrease from [H_2O] of 0.7 mol/L (**Table S3**).

In a previous kinetic study of the peroxyoxalate reaction with DNPO in aqueous DME, it was shown that the values of k_{obs} show linear correlation with the [H_2O_2], from which the hydrolysis rate constant (k_{hyd}) and the perhydrolysis rate constant (k_{per}) were calculated for different DME:H_2O mixtures (**Table S4**) [44]. These rate-constant can be employed to calculate the contribution of hydrolysis to k_{obs}, as a function of [H_2O], at 10 mmol/L H_2O_2; leading to the singlet quantum yields without influence of DNPO hydrolysis. These quantum yields reflect the efficiency of the chemiexcitation step in the media with different water content and can be directly used for the mechanistic interpretation. Values of Φ_S show an increase with the water concentration up to a value of 0.7 mol/L, followed by a steady decrease which is highly significant for higher water molarity (Fig. 2). As the quantum yields data have been corrected for loss in oxalic ester by its hydrolysis, these dependencies clearly indicate that the efficiency of the chemiexcitation step is much lower in environments with high water content. However, the data also show that small amounts of water (up to 0.7 mol/L) increase the efficiency of the chemiexcitation step in peroxyoxalate chemiluminescence.

To better understand the chemiexcitation step of the peroxyoxalate system, the reaction of DNPO with H_2O_2 catalyzed by IMI-H was studied in various water molarities using different activators such as DPA, 2,5-diphenyloxazole (PPO), perylene (PER), and rubrene (RUB). The rate constants and the singlet quantum yields were determined from the kinetic curves obtained (**Table S5**). The rate constant values in each water molarity do not depend on the nature and concentration of the activators utilized. (**Figure S4**). Singlet quantum yields can be related to the activator concentration through a double reciprocal relationship (**Equation (1)**, obtained by applying the steady-state approximation to the minimum kinetic reaction scheme of the interaction between the ACT and the high-energy intermediate [20].

$$\frac{1}{\Phi_S} = \frac{1}{\Phi_S^{\infty}} + \left(\frac{k_D}{k_{CAT}\Phi_S^{\infty}}\right)\frac{1}{[ACT]} \quad (1)$$

For all the activators used, in each water molarity studied, linear plots of the double-reciprocal relationship were obtained (Fig. 3). The slope of each correlation provides relative values for the interaction constant between the high-energy intermediate and the activator (k_{CAT}/k_D),[20] where k_{CAT} corresponds to the bimolecular rate constant for the interaction of the ACT with the HEI and k_D to the unimolecular rate constant for the unimolecular HEI decomposition. The singlet quantum yields at infinite concentration of the ACT (Φ_s^{∞}) can be obtained from the linear coefficient of the double reciprocal correlations. This quantum yield corresponds to the yield obtained under a hypothetical condition, i.e., where all HEI interacts with the activator (therefore, 'infinité ACT concentrations).

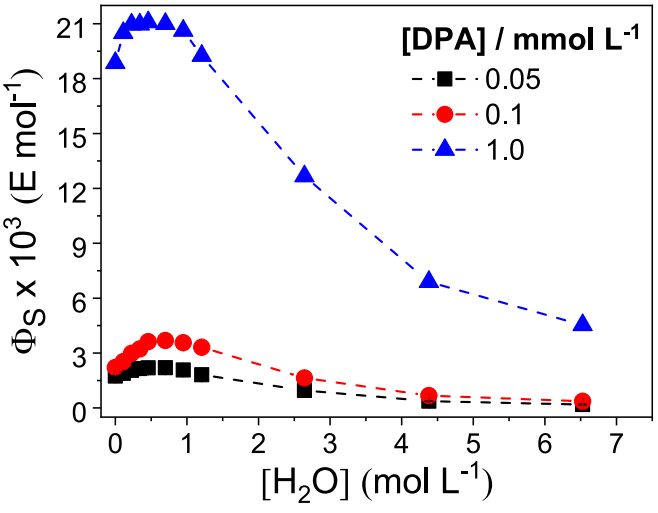

Fig. 2. Dependence of the singlet quantum yields (Φ_s) on the [H_2O], corrected for DNPO hydrolysis, in the reaction imidazole catalyzed (0.20 mmol/L) of DNPO (0.10 mmol/L) with H_2O_2 (10 mmol/L), for the three DPA concentrations.

4. Discussion

The singlet quantum yields obtained in the reaction of DNPO with hydrogen peroxide, correlated with the empirical polarity parameter $E_T(33)$, show a maximum curve with the highest quantum yield values for $E_T(33)$ values of 49 to 52, corresponding to water concentrations 0.5 to 1.2 mol/L (Fig. 4). As seen from the correlation of $E_T(33)$ with the water concentration in DME (**Figure S3**), preferential solvation of the zwitterionic ET(33) probe by water appears to occur, which should also apply to the solvation sphere around the ion pairs occurring during chemiexcitation.

To explain this experimental result, the chemiexcitation step of the peroxyoxalate reaction, which is expected to occur by the CIEEL mechanism, should be considered. For efficient formation of the electronically excited states, both the electron transfer and the electron back-transfer step must occur inside the solvent cavity **(**Scheme 2**).** If the intermediate ion radical species escape from this cage, no electron back-transfer can occur, and the products are formed in the ground state; and no light emission observed. Therefore, a possible explanation of the results of Fig. 4 can be given assuming that small amounts of water stabilize the pair of radical ions formed inside the solvent cage, and solvation initially contributes to keeping these species together until the occurrence of the electron back-transfer step, responsible for excited state formation. Increasing [water] (hence $E_T(33)$) above a certain limiting value, radical ions can be individually solvated by water molecules, thereby avoiding that these species can undergo efficient electron back-transfer, leading to a decrease in the chemiexcitation quantum yields (Scheme 2). This situation is akin to the effect of solvent polarity on the stereochemistry of the products in S_N1 reactions, where racemization/inversion, and complete racemization, may occur depending on the state of the ion pair, contact- or solvent separated, respectively [47].

The values of k_{obs} do not vary with the nature and concentration of the activator and show a slight increase with increasing [water], obtaining average k_{obs} values of 0.056 ± 0.001; 0.058 ± 0.002; 0.062 ± 0.001 and 0.069 ± 0.001 s^{-1} in water molarities of 0; 0.22; 0.7 and 1.2 mol/L, respectively (**Table S5**, **Figure S4**). This fact demonstrates that, also in these reaction media, the chemiexcitation step is much faster than the previous reaction steps and the ACT participates only in the chemiexcitation step, not in a rate-limiting reaction step [20].

Due to these facts, conventional kinetic studies cannot provide information regarding the chemiexcitation step, as this step is not rate-limiting for the reaction. However, to obtain mechanistic information about chemiexcitation, one can take advantage of the fact that the formation of electronically excited states occurs in this step. Thus, the emission intensity depends on the efficiency of excited state formation relative to other events that decompose the HEI. Therefore, by varying the nature and concentration of the ACT, it is expected that the rate of its interaction with the HEI and, consequently, the emission intensity will change. Thus, the chemiexcitation step can be studied by indirect measurement of the rate of the interaction between the activator and the HEI [20–22]. The interaction of the HEI with the ACT has been measured directly before, however, using a specific experimental arrangement, in strictly anhydrous conditions [21].

From the linear double-reciprocal correlations performed for all ACTs (Fig. 3), it is possible to determine the chemiluminescence parameters of the system in different water molarities. Higher values of the singlet quantum yield at infinite activator concentrations (Φs^{∞}) were obtained for a water concentration of 0.70 mol/L for all the activators

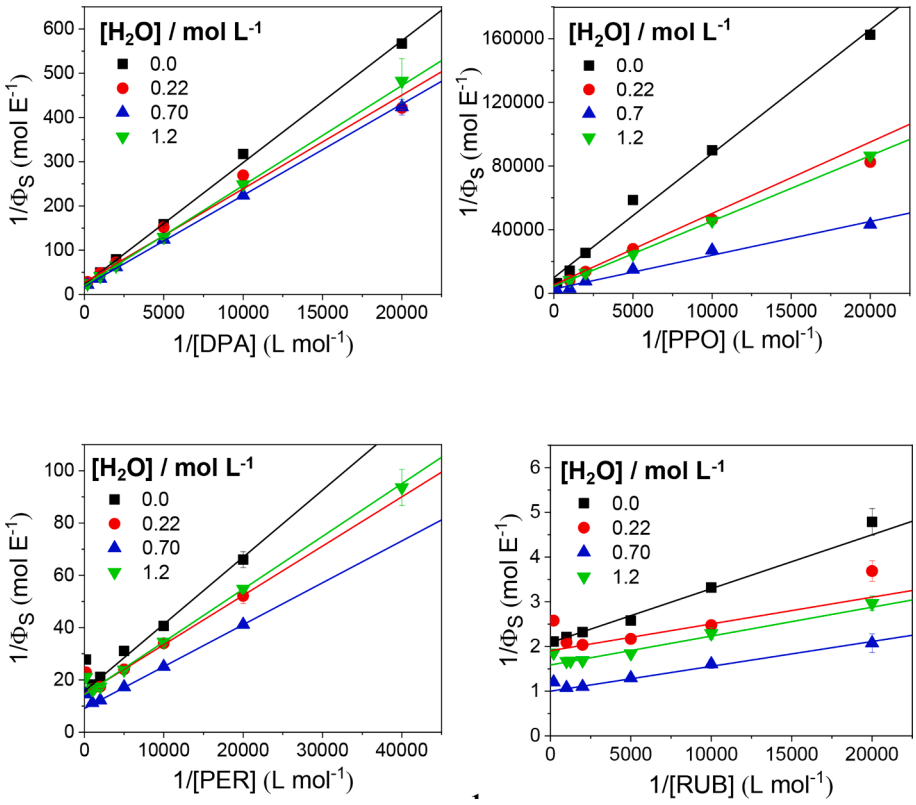

Fig. 3. Double reciprocal plot of the quantum yields and the activator concentrations (1/Φs vs. 1/[ACT]) for the reaction of DNPO (0.10 mmol/L) with H_2O_2 (10 mmol/L) catalyzed by IMI-H (0.20 mmol/L) in the presence of several activators in different DME:H_2O mixtures.

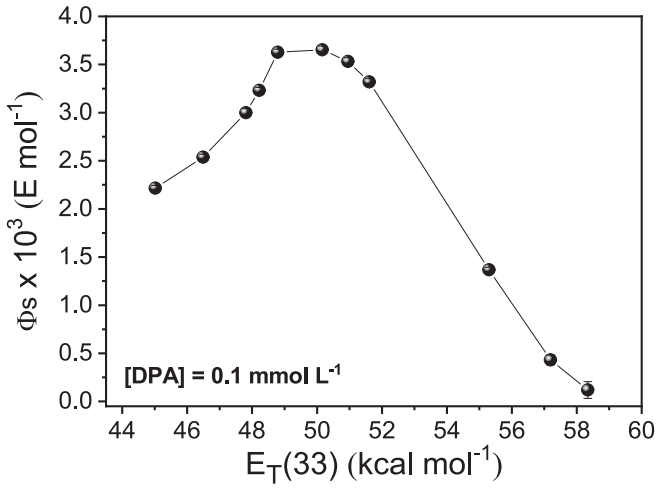

Fig. 4. Dependence on the chemiexcitation quantum yields (Φ_S) with the empirical polarity parameter $E_T(33)$ in the reaction of DNPO with hydrogen peroxide with DPA as activator. [DNPO] = 0.10 mmol/L, [IMI] = 0.2 mmol/L, [H_2O_2] = 10 mmol/L, [DPA] = 0.10 mmol/L.

studied (Table 1). The higher the value of Φs^{∞}, the higher is the probability of excited ACT (ACT*) formation from the initial radical ion pair, therefore, Φs^{∞} is directly proportional to the efficiency of excited state formation in the electron back-transfer step (Scheme 2) [20].

Furthermore, according to the CIEEL mechanism, the rate-limiting step in chemiexcitation is the electron transfer from the ACT to peroxide (k_{CAT}) and a linear correlation between the logarithm of the experimental values k_{CAT}/k_D and the activator's oxidation potential is expected, which allows the determination of the electron transfer coefficients α (**Equation (2)** [48,49].

$$\ln\left(\frac{k_{CAT}}{k_D}\right) = lnA + \alpha B - \left(\frac{\alpha}{RT}\right)E_{ox}B = \frac{e^2}{R_0 \varepsilon RT} + \frac{E_{red}}{RT} \quad (2)$$

Where A: pre-exponential factor; α: Marcus electron-transfer coefficient; R: gas constant (8,613 10^{-5} eV K^{-1}); T: temperature (K); E_{ox}: oxidation potential of the ACT; E_{red}: reduction potential of the HEI; R_0: distance between electron donor and acceptor; ε: solvent dielectric constant; e: electron charge.

For each of the water concentrations studied, a linear dependence was observed between $\ln(k_{CAT}/k_D)$ and $E_{ox}^{1/2}$ of the ACTs (Fig. 5) from which the values of the electron transfer coefficients were determined (Table 2). We should mention here that for these correlations $E_{ox}^{1/2}$ values obtained from the literature have been utilized which were not measured in the experimental conditions used in the present work. However, for our mechanistic discussion only the difference between the E_{ox} values of the ACTs is of importance and this difference should not change significantly for different media, as the ACTs are structurally similar.

The electron transfer coefficient α is related to the extent of electron transfer in the transition state; a value of 1.0 indicates an (almost) complete transfer of the electron in the transition state, while a low value (close to zero) indicates a small extension of electron transfer in the transition state [19,37,51–53].

Although the values obtained here are considerably low (Table 2), they indicate an electron transfer from ACT to peroxide as predicted by the CIEEL mechanism. These coefficients reported for various CIEEL systems are typically within the range of 0.1–0.3, including the peroxyoxalate reaction [20,21,40,54]. The α values obtained in these studies indicate an early transition state in relation to electron transfer and, presumably, also to the cleavage of the O-O bond, since these two steps must be simultaneous [21,48,49]. Interestingly, the α values show an increase with the water concentration up to 0.7 mol/L, the condition in which the highest Φ_s yields are obtained for each ACT concentration

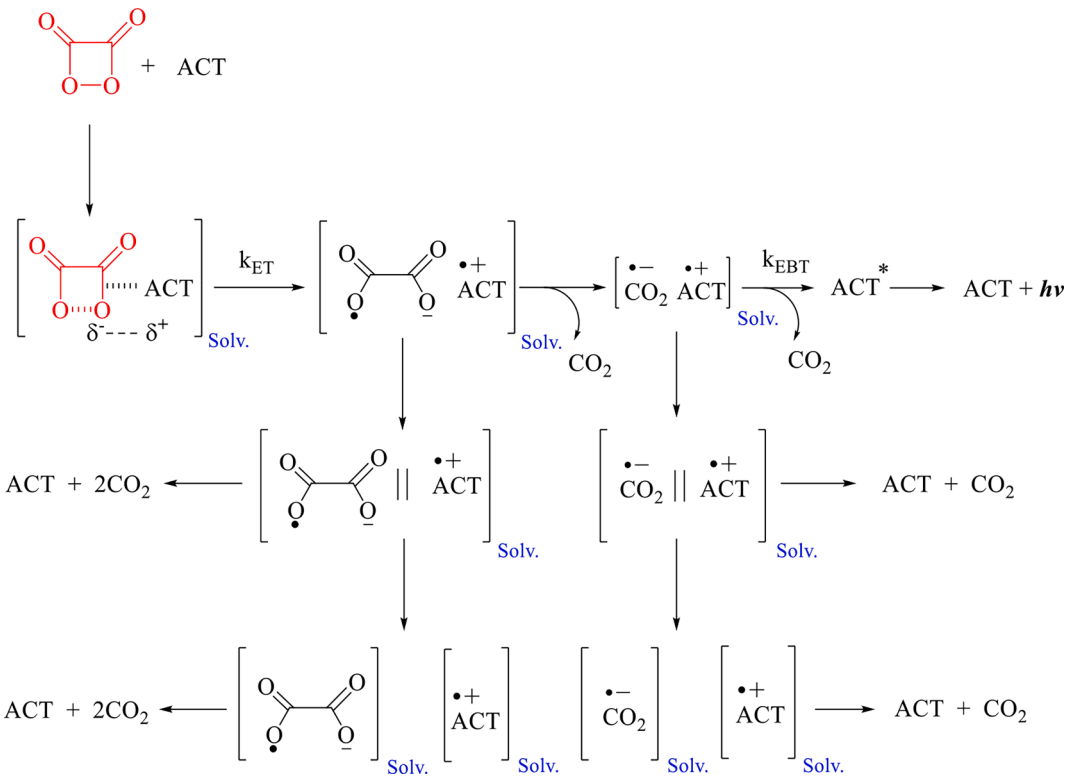

Scheme 2. Solvation process in the electron-transfer catalyzed decomposition of the HEI by its interaction with an activator (ACT).

Table 1
Chemiluminescence parameters in different water concentrations and voltametric half-peak potentials of ACTs ($E_{ox}^{1/2}$).

ACT	$E_{ox}^{1/2}$(V vs. SCE) [(a)]	[H_2O] (mol/L)	Φ_s^{∞} x 10^2 (E mol^{-1})	k_{CAT}/k_D x 10^{-3} (L/mol)
RUB	0.61	0.0	47.9 ± 0.1	17.3 ± 0.9
		0.22	52 ± 1	32 ± 6
		0.70	**100 ± 1**	18 ± 2
		1.2	63.04 ± 0.07	24 ± 2
PER	0.88	0.0	6.39 ± 0.06	6.1 ± 0.3
		0.22	6.8 ± 0.06	7.7 ± 0.4
		0.70	**11.0 ± 0.2**	5.7 ± 0.2
		1.2	6.97 ± 0.06	7.1 ± 0.1
DPA	1.06	0.0	4.4 ± 0.4	0.8 ± 0.1
		0.22	3.7 ± 0.5	1.3 ± 0.3
		0.70	**5.63 ± 0.03**	0.86 ± 0.01
		1.2	4.93 ± 0.1	0.90 ± 0.03
PPO	1.46	0.0	0.017 ± 0.007	0.6 ± 0.3
		0.22	0.018 ± 0.006	1.2 ± 0.5
		0.70	**0.06 ± 0.03**	0.6 ± 0.3
		1.2	0.022 ± 0.001	1.11 ± 0.06

[(a)] Literature values [20,50].

(**Table S5**) and also the highest values for Φ_s^{∞} (Table 1). However, α values only indicate the extent of electron transfer from the ACT to HEI in the transition state, which is determined by this transfer rate. This rate ratio k_{CAT}/k_D, should also influence the singlet quantum yields calculated for a specific concentration of ACT (Φ_s), however, the yield at "infinite concentration of ACT" (Φ_s^{∞}) does not depend on this rate, precisely due to the extrapolation of the double-reciprocal plot to zero (1/[ACT] = 0).

These results raise the following question: what are the factors that determine the infinite quantum yield? Based on the detailed CIEEL mechanism (Scheme 2), we can understand that this yield must be determined by the chemiexcitation efficiency of the electron back-transfer step, that is, the probability of forming the electronically excited state in this electron transfer (by electron transfer to ACT's LUMO) instead of ground state (by electron transfer to ACT's HOMO) [14,20,22,25]. As previously discussed, [20] this probability of chemiexcitation and, hence the value of Φ_s^{∞} must depend, primarily, on the energy released in the electron back-transfer step; this being valid for the reaction of the same HEI with structurally similar ACTs [55,56]. Following the above argument, the values of free energy released in the electron back-transfer step with formation of species in the ground (ΔG_{BET}) and excited (ΔG^*_{BET}) state for the different activators were calculated (Table 3).

As seen in Table 3, values of $|\Delta G_{EBT}|$are larger for activators with higher oxidation potentials. On the other hand, the values of $|\Delta G^*_{EBT}|$are higher for RUB and decrease with increasing oxidation potential for the other activators. Correlating ln (Φ_s^{∞}) with ΔG^*_{EBT} in each of the water concentrations, it could be noted that there is a tendency to increase the efficiency of formation of excited states with increasing $|\Delta G^*_{BET}|$ values (Fig. 6).

As previously reported, the free energy change for the electron back-transfer step was calculated based on the CIEEL scheme, so this result also contributes to confirming the mechanism.

5. Conclusions

The correction of the quantum yield values for the reaction of DNPO with H_2O_2 catalyzed by IMI-H, allows verifying the influence of water on the efficiency of the chemiexcitation step of the peroxyoxalate reaction. The increase in quantum yields for low water concentrations may be due to stabilization of the ion pairs in the CIEEL sequence, leading to an increase of the chemiexcitation efficiency. For higher [H_2O], the decrease in the quantum yields may occur due to the formation of solvent-separated ionic pairs, which can no longer undergo efficient electron back-transfer necessary for excited state formation. The linear correlation of ln (k_{CAT}/k_D) with the activator's oxidation potential supports the occurrence of an electron transfer between the ACT and the HEI.

Finally, the unexpected observation of an increase of the

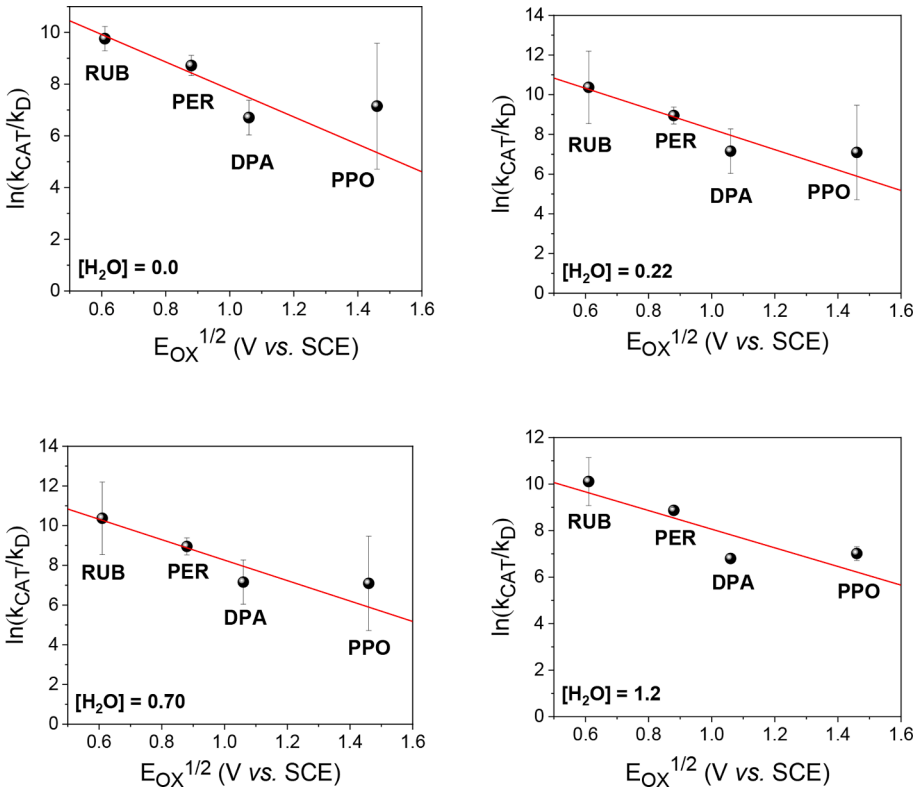

Fig. 5. Linear correlation between $\ln(k_{CAT}/k_D)$ and $E_{ox}^{1/2}$ of the activator used in the reaction of DNPO (0.10 mmol/L) with hydrogen peroxide (10 mmol/L) catalyzed by imidazole (0.20 mmol/L) in different mixtures of DME:H_2O.

Table 2
Electron transfer coefficients (α) for the imidazole catalyzed reaction of DNPO with H_2O_2 in different water molarities.

[H_2O] (mol/L)	α
0.00	0.14 ± 0.04
0.22	0.13 ± 0.05
0.70	0.13 ± 0.05
1.20	0.10 ± 0.06

Table 3
Free energy change of the electron back-transfer step between the CO_2 radical anion and the activator radical cation, together with the voltametric half-peak potential ($E_{ox}^{1/2}$) of the activators.

ACT	$E_{ox}^{1/2}$ (V vs. SCE)	ΔG_{EBT} (kJ/mol)[a]	E_s (kJ/mol)[b]	ΔG^{*c}_{EBT} (kJ/mol)[c]
RUB	0.61	−318	221	−97
PER	0.88	−344	273	−71
DPA	1.06	−362	305	−57
PPO	1.46	−400	356	−44

[a] ΔG_{EBT} = -F[$E_{ox}^{1/2}$ (ACT)–$E_{red}^{1/2}$ (CO_2)]; $E_{ox}^{1/2}$ (ACT) from Table 1, $E_{red}^{1/2}$ (CO_2) = −2,44 V [57], both vs. SHE (standard hydrogen electrode). [b] Calculated values from the maximum of the absorption and emission spectrum. [c] $-\Delta G^*_{EBT} = \Delta G_{EBT} + E_s$.

chemiexcitation efficiency in the presence of low water concentrations can be rationalized with an apparently optimum medium polarity for excited state formation, which should be used in partially aqueous systems in order to guarantee optimum sensitivity for analytical and bioanalytical applications.

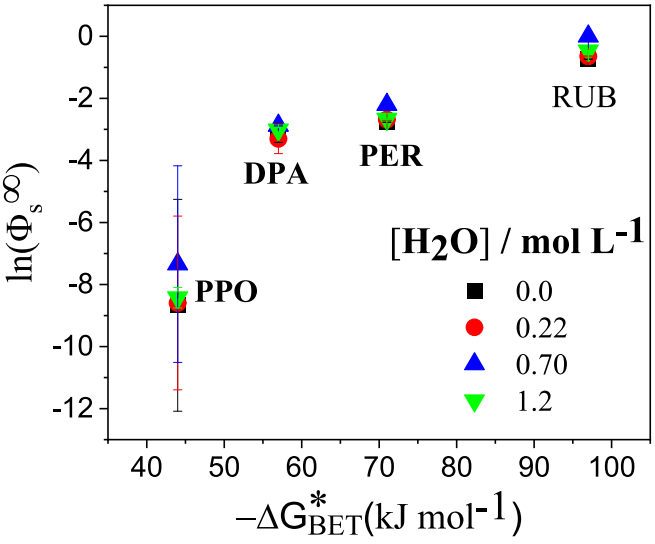

Fig. 6. Correlation between the natural logarithm of Φ_s^{∞} and the free energy change for back-electron transfer yielding excited state activators (ΔG^*_{EBT}) for the reaction of DNPO with H_2O_2 with several ACTs in various water molarities.

CRediT authorship contribution statement

Maidileyvis C. Cabello: Writing – review & editing, Writing – original draft, Visualization, Investigation, Formal analysis. **Marcos P. O. Lemos:** Investigation, Methodology. **Wilhelm J. Baader:** Writing – review & editing, Writing – original draft, Project administration, Funding acquisition, Conceptualization.

Declaration of competing interest

The authors declare that they have no known competing financial interests or personal relationships that could have appeared to influence the work reported in this paper.

Data availability

Data will be made available on request.

Acknowledgments

The authors thank the Fundação de Amparo à Pesquisa do Estado de São Paulo (FAPESP, WJB, 2014/22136-4; 2023/06417-2), Conselho Nacional de Desenvolvimento Científico e Tecnológico (CNPq, productivity fellowship 303684/2022-4 for WJB, PhD fellowship for MCC, 147138/2016-7) and Coordenadoria de Aperfeiçoamento de Pessoal de Ensino Superior (CAPES, Graduate Program of Chemistry, IQUSP (Finance Code 001)) for financial support.

Appendix A. Supplementary data

Supplementary data to this article can be found online at https://doi.org/10.1016/j.jphotochem.2024.115793.

References

[1] L. Jiang, K. Wang, Q. Kong, S. Lu, X. Chen, Research progress of chemiluminescence probes based on adamantane-dioxetane, Huagong Xuebao/CIESC J. 72 (2021) 229–246.
[2] D. Liu, C. Ju, C. Han, R. Shi, X. Chen, D. Duan, J. Yan, X. Yan, Nanozyme chemiluminescence paper test for rapid and sensitive detection of SARS-CoV-2 antigen, Biosens. Bioelectron. 173 (2021) 112817.
[3] A. Roda, S. Cavalera, F. Di Nardo, D. Calabria, S. Rosati, P. Simoni, B. Colitti, C. Baggiani, M. Roda, L. Anfossi, Dual lateral flow optical/chemiluminescence immunosensors for the rapid detection of salivary and serum IgA in patients with COVID-19 disease, Biosens. Bioelectron. 172 (2021) 112765.
[4] L. Perrin, D. Colombet, F. Ayela, Comparative study of luminescence and chemiluminescence in hydrodynamic cavitating flows and quantitative determination of hydroxyl radicals production, Ultrason. Sonochem. 70 (2021) 105277.
[5] J.C. Domínguez-Romero, B. Gilbert-López, M. Beneito-Cambra, A. Molina-Díaz, Renewable chemiluminescence optosensors based on implementation of bead injection principle with multicommutation, Talanta 182 (2018) 267–272.
[6] M. Mirasoli, A. Buragina, L.S. Dolci, M. Guardigli, P. Simoni, A. Montoya, E. Maiolini, S. Girotti, A. Roda, Development of a chemiluminescence-based quantitative lateral flow immunoassay for on-field detection of 2,4,6-trinitrotoluene, Anal. Chim. Acta 721 (2012) 167–172.
[7] M.C. Cabello, F.H. Bartoloni, E.L. Bastos, W.J. Baader, The molecular basis of organic chemiluminescence, Biosensors (Basel) 13 (2023) 452.
[8] E.A. Chandross, A new chemiluminescent system, Tetrahedron Lett. 12 (1963) 761–765.
[9] R.A. Rauhut, M.M. Bollyky, L.J. Roberts, B.G. Loy, M. Whitman, R.H. Iannotta, A. V. Semsel, A.M. Clarke, Chemiluminescence from reactions of electronegatively substituted aryl oxalates with hydrogen peroxide and fluorescent compounds, J. Am. Chem. Soc. 89 (1967) 6515–6522.
[10] M.M. Rauhut, Chemiluminescence from concerted peroxide decomposition reactions, Acc. Chem. Res. 2 (1969) 80–87.
[11] A.M. Rauhut, M.M. Sheehan, D. Clarke, R.A. Semsel, Structural criteria for chemiluminescence in acyl peroxide decomposition reactions, Photochem. Photobiol. 4 (6) (1965) 1097–1110.
[12] S.M. Silva, A.P. Lang, A.P.F. dos Santos, M.C. Cabello, L.F.M.L. Ciscato, F. H. Bartoloni, E.L. Bastos, W.J. Baader, Cyclic peroxidic carbon dioxide dimer fuels peroxyoxalate chemiluminescence, J. Org. Chem. 86 (2021) 11434–11441.
[13] D. Gerbig, P.R. Schreiner, Preparation and spectroscopic identification of the cyclic CO_2 dimer 1,2-dioxetanedione, J. Am. Chem. Soc. 145 (2023) 22341–22346.
[14] L.F.M.L. Ciscato, F.A. Augusto, D. Weiss, F.H. Bartoloni, S. Albrecht, H. Brandl, T. Zimmermann, W.J. Baader, The chemiluminescent peroxyoxalate system: State of the art almost 50 years from its discovery, ARKIVOC 2012 (2012) 391–430.
[15] S.M. Silva, F. Casallanovo, K.H. Oyamaguchi, L.F.L.M. Ciscato, C.V. Stevani, W. J. Baader, Kinetic studies on the peroxyoxalate chemiluminescence reaction: Determination of the cyclization rate constant, Luminescence 17 (2002) 313–320.
[16] C.V. Stevani, I.P.D.A. Campos, W.J. Baader, Synthesis and characterisation of an intermediate in the peroxyoxalate chemiluminescence: 4-chlorophenyl O, O-hydrogen monoperoxy-oxalate, J. Chem. Soc. Perkin Trans. 2 (1996) 1645–1648.
[17] C.V. Stevani, D.F. Lima, V.G. Toscano, W.J. Baader, Kinetic studies on the peroxyoxalate chemiluminescent reaction: Imidazole as a nucleophilic catalyst, J. Chem. Soc. Perkin Trans. 2 (1996) 989–995.
[18] C.V. Stevani, W.J. Baader, Kinetic studies on the chemiluminescent decomposition of an isolated intermediate in the peroxyoxalate reaction, J. Phys. Org. Chem. 10 (1997) 593–599. .
[19] G.B. Schuster, Chemiluminescence of organic peroxides. Conversion of ground-state reactants to excited-state products by the chemically initiated electron-exchange luminescence mechanism, Acc. Chem. Res. 12 (1979) 366–373.
[20] C.V. Stevani, S.M. Silva, W.J. Baader, Studies on the mechanism of the excitation step in peroxyoxalate chemiluminescence, Eur. J. Org. Chem. (2000) 4037–4046.
[21] L.F.M.L. Ciscato, F.H. Bartoloni, E.L. Bastos, W.J. Baader, Direct kinetic observation of the chemiexcitation step in peroxyoxalate chemiluminescence, J. Org. Chem. 74 (2009) 8974–8979.
[22] S.M. Silva, K. Wagner, D. Weiss, R. Beckert, C.V. Stevani, W.J. Baader, Studies on the chemiexcitation step in peroxyoxalate chemiluminescence using steroid-substituted activators, Luminescence 17 (2002) 362–369.
[23] M. Vacher, I. Fdez, B.-W. Galván, S. Ding, R. Schramm, P. Berraud-Pache, N. Naumov, Y.-J. Ferré, I. Liu, D. Navizet, W.J. Roca-Sanjuán, R.L. Baader, Chemi- and bioluminescence of cyclic peroxides, Chem. Rev. 118 (2018) 6927–6974.
[24] W.J. Baader, C.V. Stevani, E.L. Bastos, Chemiluminescence of Organic Peroxides, in: Z. Rappoport (Ed.), The Chemistry of Peroxides, Wiley-VCH, Chichester, 2006, pp. 1211–1278.
[25] E.L. Bastos, P. Farahani, E.J.H. Bechara, W.J. Baader, Four-membered cyclic peroxides: Carriers of chemical energy, J. Phys. Org. Chem. 30 (2017) 1–18.
[26] Z. Li, Z. Li, D. Li, H. Gao, X. Chen, L. Cao, Y. Hou, Molecularly imprinted polymer-based chemiluminescence imaging assay for the determination of ethopabate residues in chicken muscle, Anal. Methods 00 (2015) 1–9.
[27] S. Sadeghi Mohammadi, Z. Vaezi, B. Shojaedin-Givi, H. Naderi-Manesh, Chemiluminescent liposomes as a theranostic carrier for detection of tumor cells under oxidative stress, Anal. Chim. Acta 1059 (2019) 113–123.
[28] Y. Yan, P. Shi, W. Song, S. Bi, Chemiluminescence and bioluminescence imaging for biosensing and therapy: In vitro and in vivo perspectives, Theranostics 9 (2019) 4047–4065.
[29] H.M. Hu, X.F. Yin, X.Z. Wang, H. Shen, A study on the system of nonaqueous microchip electrophoresis with on-line peroxyoxalate chemiluminescence detection, J. Sep. Sci. 36 (2013) 713–720.
[30] D. Chen, R. Peng, H. Zhou, H. Liu, Sensitive determination of 4-nitrophenol based on its enhancement of a peroxyoxalate chemiluminescence system containing graphene oxide quantum dots and fluorescein, Microchim Acta 183 (2016) 1699–1704.
[31] L. Delafresnaye, F.R. Bloesser, K.B. Kockler, C.W. Schmitt, I.M. Irshadeen, C. Barner-Kowollik, All eyes on visible-light peroxyoxalate chemiluminescence read-out systems, Chem. Eur. J. 26 (2020) 114–127.
[32] M. Wada, N. Kuroda, Chromatographic determination of low-molecular mass unsaturated aliphatic aldehydes with peroxyoxalate chemiluminescence detection after fluorescence labeling with, J. Chromatog. B 953–954 (2014) 147–152.
[33] F.H. Bartoloni, L.F.M.L. Ciscato, M.M. De Medeiros Peixoto, A.P.F. Dos Santos, C. Da Silva Santos, S. De Oliveira, F.A. Augusto, A.P.E. Pagano, W.J. Baader, E. L. Bastos, Luz: Um raro produto de reação, Quim Nova 34 (2011) 544–554.
[34] A. Tahirović, A. Čopra, E. Omanović-Mikličanin, K. Kalcher, A chemiluminescence sensor for the determination of hydrogen peroxide, Talanta 72 (2007) 1378–1385.
[35] M.C. Cabello, G.A. Souza, L.V. Bello, W.J. Baader, Mechanistic studies on the salicylate-catalyzed peroxyoxalate chemiluminescence in aqueous medium, Photochem. Photobiol. 96 (2020) 28–36.
[36] F.A. Augusto, F.H. Bartoloni, M.C. Cabello, A.P.F. dos Santos, J.W. Baader, Kinetic studies on 2,6-lutidine catalyzed peroxyoxalate chemiluminescence in organic and aqueous medium: Evidence for general base catalysis, J. Photochem. Photobiol. 382 (2019) 111967.
[37] M.C. Cabello, O.A.A. El Seoud, W.J. Baader, Effect of ionic liquids on the kinetics and quantum efficiency of peroxyoxalate chemiluminescence in aqueous media, J. Photochem. Photobiol. A Chem. 367 (2018).
[38] G.A. Souza, M.M.M. Peixoto, A.P.F. Santos, W.J. Baader, General acid and base catalysis by phosphate in peroxyoxalate chemiluminescence, Chemistry Select 1 (2016) 2307–2315.
[39] F.A. Augusto, F.H. Bartoloni, A.P.E. Pagano, W.J. Baader, Mechanistic study of the peroxyoxalate system in completely aqueous carbonate buffer, Photochem. Photobiol. 97 (2020) 309–316.
[40] M.C. Cabello, L.V. Bello, W.J. Baader, Use of coumarin derivatives as activators in the peroxyoxalate system in organic and aqueous media, J. Photochem. Photobiol. A Chem. 408 (2020) 113076.
[41] J.J. DeCorpo, A. Baronavski, M.V. McDowell, F.E. Saalfeld, Formation of carbon dioxide dimer in chemiluminescent reactions, J. Am. Chem. Soc. 94 (1972) 2879–2880.
[42] C.L.R. Catherallt, T.F. Palmer, Determination of absolute chemiluminescence quantum yields for reactions of bis-(pentachlorophenyl) oxalate, hydrogen peroxide and fluorescent compounds, J. Biolumin. Chemilumin. 3 (1989) 147–154.
[43] S.P. Souza, M. Khalid, F.A. Augusto, W.J. Baader, Peroxyoxalate chemiluminescence efficiency in polar medium is moderately enhanced by solvent viscosity, J. Photochem. Photobiol. A: Chem. 321 (2016) 143–150.
[44] M.C. Cabello, J.W. Baader, Water effect on peroxyoxalate kinetics and mechanism for oxalic esters with distinct reactivities, Photochem. Photobiol. 97 (2021) 1023–1031.
[45] M.L. Cotton, H.B. Dunford, Studies on horseradish peroxidase. XI. On the nature of compounds I and II as determined from the kinetics of the oxidation of ferrocyanide, Can J. Chem. 51 (1973) 582–587.
[46] C. Reichardt, Solvents and solvent effects in organic chemistry, third ed., Wiley-VCH, Weinheim, Germany, 2003, p. 629.

[47] J. Clayden, N. Greeves, S. Warren, Organic chemistry, second ed., Oxford University Press, London, 2012.
[48] R.A. Marcus, Chemical and electrochemical electron-transfer theory, Annu. Rev. Phys. Chem. 15 (1964) 155.
[49] F. Scandola, V. Balzani, G.B. Schuster, Free-energy relationships for reversible and irreversible electron-transfer processes, J. Am. Chem. Soc. 103 (1981) 2519–2523.
[50] S. Doose, H. Neuweiler, M. Sauer, Fluorescence quenching by photoinduced electron transfer: A reporter for conformational dynamics of macromolecules, Chem. Phys. Chem. 10 (2009) 1389–1398.
[51] W. Adam, O. Cueto, Fluorescer-enhanced chemiluminescence of α-peroxylactones via electron exchange, J. Am. Chem. Soc. 101 (1979) 6511–6515.
[52] J. Young Koo, G.B. Schuster, Chemiluminescence of diphenoyl peroxide. Chemically initiated electron exchange luminescence. A new general mechanism for chemical production of electronically excited states, J. Am. Chem. Soc. 100 (1978) 4496–4503.
[53] G. Burton, H. Nordlóv, S. Hosozawa, H. Matsumoto, P.M. Jordan, P.E. Eagerness, L. M. Pryde, A.I. Scott, P.M. Jordan, G. Burton, H. Nordlóv, M. Schneider, L.M. Pryde, Investigation of the mechanism of the unimolecular and the electron-donor-catalyzed thermal fragmenta- tion of secondary peroxy esters. Chemiluminescence of 1- phenylethyl peroxyacetate by the chemically initiated electron- exchange luminescence mechanism, J. Am. Chem. Soc. 101 (1979) 3116–3118.
[54] J. Alves, A. Boaro, J.S. Da Silva, T.L. Ferreira, V.B. Keslarek, C.A. Cabral, R. B. Orfão, L.F.M.L. Ciscato, F.H. Bartoloni, Lophine derivatives as activators in peroxyoxalate chemiluminescence, Photochem. Photobiol. Sci. 14 (2014) 320–328.
[55] F.H. Bartoloni, M.A. De Oliveira, L.F.M.L. Ciscato, F.A. Augusto, E.L. Bastos, W. J. Baader, Chemiluminescence efficiency of catalyzed 1,2-dioxetanone decomposition determined by steric effects, J. Org. Chem. 80 (2015) 3745–3751.
[56] F.A. Augusto, A. Francés-Monerris, I. Fdez Galván, D. Roca-Sanjuán, E.L. Bastos, W. J. Baader, R. Lindh, Mechanism of activated chemiluminescence of cyclic peroxides: 1,2-dioxetanes and 1,2-dioxetanones, Phys. Chem. Chem. Phys. 19 (2017) 3955–3962.
[57] M.M. Chang, T. Saji, A.J. Bard, E. Chemiluminescence, 30. Electrochemical oxidation of oxalate ion in the presence of luminescers in acetonitrile solutions, J. Am. Chem. Soc. 99 (1977) 5399–5403.